BIOCHEMISTRY
including biophysical chemistry & molecular biology

Article

pubs.acs.org/biochemistry

Properties of the Monomeric Form of Human 14-3-3ζ Protein and Its Interaction with Tau and HspB6

Nikolai N. Sluchanko,[†] Maria V. Sudnitsyna,[†] Alim S. Seit-Nebi,[†] Alfred A. Antson,[‡] and Nikolai B. Gusev*[,†]

[†]Department of Biochemistry, School of Biology, Moscow State University, Moscow 119991, Russian Federation

[‡]York Structural Biology Laboratory, Department of Chemistry, University of York, York YO10 5YW, United Kingdom

Supporting Information

ABSTRACT: Dimers formed by seven isoforms of the human 14-3-3 protein participate in multiple cellular processes. The dimeric form has been extensively characterized; however, little is known about the structure and properties of the monomeric form of 14-3-3. The monomeric form is involved in the assembly of homo- and heterodimers, which could partially dissociate back into monomers in response to phosphorylation at Ser58. To obtain monomeric forms of human 14-3-3ζ, we produced four protein constructs with different combinations of mutated (M) or wild-type (W) segments E^{5}, $^{12}LAE^{14}$, and $^{82}YREKIE^{87}$. Under a wide range of expression conditions in *Escherichia coli*, the MMM and WMM mutants were insoluble, whereas WMW and MMW mutants were soluble, highly expressed, and purified to homogeneity. WMW and MMW mutants remained monomeric over a wide range of concentrations while retaining the α-helical structure characteristic of wild-type 14-3-3. However, WMW and MMW mutants were highly susceptible to proteolysis and had much lower thermal stabilities than the wild-type protein. Using WMW and MMW mutants, we show that the monomeric form interacts with the tau protein and with the HspB6 protein, in both cases forming complexes with a 1:1 stoichiometry, in contrast to the 2:1 and/or 2:2 complexes formed by wild-type 14-3-3. Significantly, this interaction requires phosphorylation of tau protein and HspB6. Because of minimal changes in structure, MMW and especially WMW mutant proteins are promising candidates for analyzing the effect of monomerization on the physiologically important properties of 14-3-3ζ.

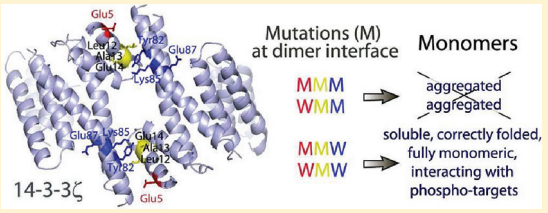

Many different processes in eukaryotic cells are regulated by phosphorylation of serine and/or threonine. 14-3-3 proteins recognize characteristic phosphorylated consensus motifs RX_{2-3}[pS/pT]X[P/G][1] within the polypeptide chain or [pS/pT]X_{1-2}-COOH[2] at the C-terminus. Being able to interact with more than 300 different target partners,[3] 14-3-3 proteins participate in the regulation of diverse and important events like proliferation, apoptosis, replication, signal transduction, etc.

The members of the 14-3-3 family are ubiquitously expressed in eukaryotes and are usually present as several isoforms.[4,5] Seven distinct genes encode human 14-3-3 isoforms (β, γ, σ, τ/θ, η, ζ, and ε) that usually form homo- and heterodimers.[6] The X-ray crystallographic data indicate that 14-3-3 has a horseshoe or a clamplike shape and is composed of two monomers each containing nine antiparallel α-helices.[7] Approximately 70% of the residues are involved in the formation of α-helices,[4,8,9] which makes 14-3-3 molecules highly stable. Monomers of 14-3-3 interact with each other by their N-terminal parts comprising α-helices 1−4, whereas C-terminal halves make up the side walls of the clamp.[5,7] Each subunit contains a special site for phosphorylated peptide binding;[10] however, certain unphosphorylated proteins can also interact with 14-3-3.[11−13]

Dimers are considered the main functional unit of 14-3-3. The dimeric structure appears to play an important role in the regulation of Raf kinase,[14] p53 transcriptional activity,[15] and specific Raf and DAF-16 binding.[16] Scaffolding function, i.e., the ability of 14-3-3 to bridge two different partners mediating their interaction,[17] is also absolutely dependent on the dimeric structure of 14-3-3. The stability of 14-3-3 dimers seems to be regulated by phosphorylation of Ser58 located at the subunit interface. The effect of Ser58 phosphorylation on the 14-3-3 quaternary structure remained controversial for some time.[18−20] However, recently published data indicate that the S58E mutation mimicking phosphorylation, as well as phosphorylation itself, leads to significant destabilization and provokes partial dissociation of 14-3-3 dimers upon dilution.[8,20−24] The resulting monomers might be important for assembly of heterodimers consisting of different 14-3-3 isoforms, for modulation of the interaction of 14-3-3 with different target proteins, and for the scaffolding function of 14-3-3. However, incomplete dissociation of dimers induced by phosphorylation or by a mutation mimicking phosphorylation hampers the capture of 14-3-3 monomers, investigation of their properties, and interaction with target proteins that remains one of the most intriguing questions concerning 14-3-3 biology.

Received: August 31, 2011
Revised: September 27, 2011
Published: October 6, 2011

Dimer-deficient mutants of 14-3-3 were previously expressed in the cells and used for investigation of Raf-kinase regulation,[14] Raf and DAF-16 binding,[16] and functioning of Ca^{2+}-dependent K^+ channels.[25] The stability of dimer-deficient 14-3-3 mutants was also analyzed in vivo.[26] However, the structure and properties of these mutants, usually containing a number of nonconservative replacements, were not carefully analyzed, thus leaving open the question of whether such mutants were adequately folded.

This study is focused on obtaining correctly folded monomeric forms of 14-3-3ζ and analysis of their biochemical properties. We also investigated interaction of monomeric forms of 14-3-3ζ with the fetal isoform of human tau protein and human small heat shock protein HspB6 (Hsp20).

MATERIALS AND METHODS

Molecular Cloning and Protein Expression and Purification. cDNA encoding wild-type human 14-3-3ζ cloned into the pET23b vector using *Nde*I and *Xho*I restriction sites was used as a template for generating the monomeric mutants.[8] Three sites, namely, E^5, ^{12}LAE^{14}, and ^{82}YREKIE^{87}, were subjected to mutation. Each of these sites is designated either W (wild type, not mutated) or M (mutated). Mutant cDNA corresponding to 14-3-3ζ with dimerization blocking substitutions $E^5 \rightarrow K^5$, ^{12}LAE$^{14} \rightarrow {}^{12}$QQR^{14}, and ^{82}YREKIE$^{87} \rightarrow {}^{82}$QRENIQ^{87} (the so-called MMM mutant,[14] containing seven underlined replacements) was obtained in two steps by the megaprimer method[27] using the T7 promotor (forward) and the following reverse primers: 5′ CTCAGCCTGCCGCTGCTGTTTGGCCTTCTGAACCAGCTTATTTTTATC 3′ for $E^5 \rightarrow K^5$ and ^{12}LAE$^{14} \rightarrow {}^{12}$QQR^{14} and 5′ CTTAGCTCCGTCTGAATGTTCTCTCTCTGTTCTCGAGC 3′ for ^{82}YREKIE$^{87} \rightarrow {}^{82}$QRENIQ^{87} substitutions (mutated codons and residues are underlined). The WMM mutant with E^5 left unchanged was obtained accidentally. WMW and MMW mutants were obtained by replacing the mutated region of WMM and MMM mutants encoding sequence ^{82}QRENIQ^{87} with the wild-type sequence. The S58E mutant of 14-3-3 was obtained previously.[28] Full-length cDNAs of untagged human small heat shock protein HspB6 (Hsp20) and fetal tau protein were cloned as described previously.[29,30] In all cases, the presence of mutations and the integrity of the coding sequence were confirmed by DNA sequencing.

DNA constructs with appropriate inserts were used for transformation of *Escherichia coli* BL21(DE3)Rosetta or BL21(DE3)pLysS cells made competent by chemical treatment.[31] Expression of target proteins was induced by 0.1−1 mM isopropyl β-D-thiogalactoside (IPTG) and lasted for 2−4 h at 20−37 °C. Alternatively, the proteins were expressed by incubation in 3×LB (Luria-Bertani, Amresco) medium without IPTG for 8 h at 37 °C followed by incubation for 12−16 h at 20−30 °C. This method of autoinduction was successfully used for expression of a wide number of different proteins,[32] and we found it very effective for the high-yield expression of HspB6. The cells were harvested by centrifugation, resuspended in lysis buffer, and subjected to sonication. The solubility of the expressed proteins was analyzed by SDS gel electrophoresis.[33]

All proteins were purified as described previously[8,28] using ammonium sulfate fractionation followed by ion-exchange and size-exclusion chromatography. HspB6 was purified as described previously.[34] The purified proteins were dialyzed against buffer B [20 mM Tris-acetate (pH 7.6), 10 mM NaCl, 0.1 mM EDTA, 0.1 mM PMSF, and 15 mM ME], concentrated by ultrafiltration, and stored frozen at −20 °C. Protein concentrations were determined spectrophotometrically.[28] The recombinant His-tagged catalytic subunit of mouse cAMP-dependent protein kinase was obtained as described previously.[30] All proteins were homogeneous according to sodium dodecyl sulfate−polyacrylamide gel electrophoresis (SDS−PAGE).[33]

Circular Dichroism (CD) Spectroscopy of 14-3-3. 14-3-3ζ or its WMW and MMW mutants (0.76 mg/mL) were dialyzed overnight against 50 mM phosphate (pH 7.5) containing 150 mM NaCl and 0.2 mM DTT. Far-UV CD spectra were recorded in a 0.2 mm cell at 20 °C in the range of 190−260 nm. CD spectra were recorded at a rate of 0.5 nm/min on a Chirascan circular dichroism spectrometer (Applied Photophysics). The data presented are averages of five accumulations.

Isoelectric Focusing of 14-3-3. The samples of wild-type 14-3-3 and its mutants were subjected to isoelectric focusing in 5% polyacrylamide gels containing 8.5 M urea, 0.02% Triton X-100, and 0.4% ampholines (pH 3−10) and 1.6% ampholines (pH 5−7). H_3PO_4 (10 mM) and NaOH (20 mM) were used as electrode buffers. After electrofocusing (3 h at 500 V), the gels were fixed in a solution containing 4% sulfosalicylic acid, 12% trichloroacetic acid, and 30% ethanol, washed in a solution containing 10% acetic acid and 30% ethanol, and stained with Coomassie R-250.

Analytical Size-Exclusion Chromatography and Multi-angle Laser Light Scattering. The samples (150 μL) containing 1.5−175 μg of analyzed protein or protein standards were subjected to size-exclusion chromatography on a Superdex 200 HR 10/30 column equilibrated with 20 mM Tris-acetate (pH 7.6) containing 150 mM NaCl, 5 mM $MgCl_2$, 0.1 mM PMSF, and 15 mM ME and operated at a flow rate of 0.5 mL/min. The Stokes radius (R_s) was calculated from the calibration curve showing the dependence of $[-\log(K_{av})]^{0.5}$ on the Stokes radii of protein standards [aldolase (48.1 Å), bovine serum albumin (35.4 Å), ovalbumin (30.5 Å), chymotrypsinogen (20.9 Å), and RNase (16.4 Å)].

To determine molecular mass of the 14-3-3 monomer, we loaded the sample (50 μL) of the WMW mutant (0.5−6.0 mg/mL) on a BioSep-SEC-S3000 column connected to a DAWN HELEOS II multiangle laser light scattering detector and an Optilab T-rEX refractometer (Wyatt Technology, Santa Barbara, CA) and eluted the column with 20 mM Tris-HCl buffer (pH 7.5) containing 100 mM NaCl, 0.5 mM EDTA, and 1 mM DTT at a flow rate of 1 mL/min. The data from the detectors were processed in Astra version 5.3.4 (Wyatt Technology) to yield the final profiles.

Limited Trypsinolysis of 14-3-3. Limited proteolysis of 14-3-3ζ and its mutants (0.5 mg/mL) was performed in buffer T1 [30 mM Tris-acetate (pH 7.5), 10 mM NaCl, 3 mM EDTA, and 15 mM ME]. Trypsinolysis was performed at 37 °C for 0−1.5 h at a 14-3-3ζ:TPCK-treated trypsin weight ratio of 150:1. Reaction was stopped by addition of PMSF, and the protein composition of samples thus obtained was analyzed by 15% SDS−PAGE.[33]

Intrinsic Tryptophan Fluorescence and Thermal Stability of 14-3-3. Fluorescence spectra of wild-type 14-3-3ζ and its mutants (0.02−0.2 mg/mL) were recorded on a Cary Eclipse spectrofluorometer (Varian Inc.) as described previously.[8] Fluorescence was excited at 295 nm and recorded in the 300−400 nm range with a 5 nm slit width. The thermal stability of 14-3-3 and its mutants (0.07 mg/mL) was analyzed

by recording the dependence of the fluorescence intensity (excitation at 295 nm and emission at 320 and 365 nm) on temperature. The protein samples were heated in an automatic Peltier cell holder of the Cary Eclipse spectrofluorometer from 40 to 75 °C and cooled with constant rate of 1 °C/min. The dependence of completeness of thermal transition (parameter α)[8,35] or parameter A (ratio of fluorescence at 320 and 365 nm) on temperature was estimated as described previously.[36] The final plots were used for determination of half-transition temperatures that reflect the thermal stability of the analyzed proteins.

Binding of Bis-ANS to 14-3-3. Hydrophobic properties of 14-3-3 and its mutants were analyzed via titration of a protein solution (1 μM) with hydrophobic probe bis-ANS (final concentrations of 0−12 μM). After addition of each portion of bis-ANS, we recorded fluorescence spectra in the range of 310−575 nm (excitation at 295 nm) and the intensity of bis-ANS fluorescence excited at 385 nm and recorded at 495 nm (5 nm slit width). All measurements were performed at 25 °C on a Cary Eclipse spectrofluorometer (Varian Inc.). Fluorescence resonance energy transfer (FRET) from excited Trp residues to bound bis-ANS was reflected by a decrease in the intrinsic Trp fluorescence at 340 nm with a concomitant increase in the fluorescence of bis-ANS at 495 nm.

Phosphorylation of Tau Protein and HspB6 by PKA. Phosphorylation of proteins was performed as described previously.[28] Briefly, tau protein (10−12 μM) was incubated in buffer P containing 20 mM Tris-HCl (pH 7.5), 10 mM glycerol 1-phosphate, 1 mM $MgCl_2$, 0.1 mM PMSF, 15 mM ME, 150−250 μM ATP, and trace amounts of [γ-^{32}P]ATP in the presence of protein kinase A (PKA) for 4 h at 37 °C. After the incubation mixture had been heated to 90 °C for 5 min, inactivated and denatured protein kinase was removed by centrifugation at 14000g.[28] Incorporation of radioactive phosphate was detected on the RackBeta 1214 (LKB) scintillation counter as described previously.[28] Under the conditions that were used, the extent of phosphorylation was in the range of 1.5−2.0 mol of phosphate/mol of tau protein, which is similar to results reported previously.[30,37]

Phosphorylation of HspB6 (50 μM) was performed under similar conditions at 37 °C for 1 h and was accompanied by incorporation of ∼0.80−0.95 mol of phosphate/mol of HspB6, in good agreement with previously published data.[38]

Analysis of Protein−Protein Interaction. Gel electrophoresis under nondenaturing conditions in a slightly modified Schaub and Perry system[39] was performed as described previously.[28] Samples containing isolated 14-3-3ζ (or its mutants), isolated phosphorylated tau protein, or mixtures of 14-3-3 with tau protein were incubated for 30−40 min at 37 °C, loaded on 15% polyacrylamide gels containing 15% glycerol, and subjected to electrophoresis, which was conducted for 120−180 min at room temperature. Alternatively, isolated phosphorylated HspB6, isolated 14-3-3ζ, or their mixture was incubated for 20−30 min at 37 °C in buffer B in the presence of 1 mM $MgCl_2$.[28] The protein samples were subjected to native gel electrophoresis[39] on an 18% polyacrylamide gel that was run in the presence of 1 mM $MgCl_2$ for 18 h at room temperature. After being stained with Coomassie R-250, the gels were subjected to densitometry and autoradiography (if necessary).

Chemical cross-linking with glutaraldehyde (GA) was used for further investigation of protein−protein interactions. The samples containing isolated proteins or their mixtures were incubated for 15 min at 30 °C with GA (final concentration of 0.05%). Reaction was stopped by addition of SDS sample buffer, and the protein composition of samples was analyzed via 5 to 20% gradient SDS−PAGE.[30] All gels were stained with Coomassie R-250 and subjected to quantitative densitometry and autoradiography (if necessary).

Size-exclusion chromatography on a Superdex 200 HR 10/30 column was used to analyze the interaction of wild-type 14-3-3 or its mutants with HspB6. Qualitative comparison of the interaction of HspB6 with different 14-3-3 mutants was performed as follows. Samples (150 μL) containing isolated 14-3-3 species (final concentration of 0.7 mg/mL), phosphorylated or unphosphorylated isolated HspB6 (final concentration of 0.5 mg/mL), or their mixture in buffer SE [20 mM Tris-acetate (pH 7.6), 150 mM NaCl, 0.1 mM EDTA, 0.1 mM PMSF, and 15 mM ME] was subjected to the size-exclusion chromatography on a Superdex 200 HR 10/30 column that was preliminarily calibrated with protein markers [ferritin (440 kDa), catalase (232 kDa), rabbit skeletal glyceraldehyde phosphate dehydrogenase (144 kDa), bovine serum albumin (68 kDa), and ovalbumin (43 kDa)]. Quantitative determination of apparent dissociation constants of the complexes formed by 14-3-3 mutants and phosphorylated HspB6 was performed as follows. The samples (150 μL) containing a fixed concentration of HspB6 (25 μM per monomer) and variable quantities of different species of 14-3-3 (0−60 μM per monomer) were preincubated for 30 min at 37 °C in buffer SE and subjected to SEC on a Superdex 200 HR 10/30 column. Chromatography was performed at a flow rate of 0.5 mL/min, and 300 μL fractions were collected and analyzed by SDS gel electrophoresis. In addition, each fraction was counted on a RackBeta 1214 (LKB) scintillation counter. Calculating the radioactivity of the peak corresponding to isolated phosphorylated HspB6 while knowing the total radioactivity of the sample loaded on the column and total concentrations of 14-3-3 and HspB6 in the mixture allowed estimation of the apparent binding constants for binding of different 14-3-3 species to phosphorylated HspB6.

RESULTS

Design of Monomeric Mutants of 14-3-3ζ. The first dimer-deficient (nontruncated) mutant of 14-3-3, constructed by Tzivion et al. for investigation of the role of 14-3-3 monomers in Raf regulation,[14] contained seven mutations predominantly located at the intersubunit surface of the 14-3-3 dimer (Figure 1). Each mutated motif (residue 5, residues 12−14, and residues 82−87) was marked either W (wild-type) or M (mutated), starting from the N-terminus. Thus, the dimer-deficient mutant of Tzivion et al.[14] can be denoted MMM. Not all of these residues (for instance, Glu14 and Glu87) seem to be directly involved in formation of the intersubunit surface (Figure 1); however, it was supposed that mutation of all these residues is important for 14-3-3 monomerization.[14] Analogous mutants of the WMM, WWM, or WMW type were used in a number of other investigations.[16,25,26] All these investigations were performed at a cellular level without previous detailed investigation of physicochemical properties of these mutants and without verification of the correctness of their folding.

Initially, we constructed an MMM mutant of 14-3-3 and tried to express it in *E. coli*. Although we used a number of different conditions (induction by IPTG and autoinduction, wide ranges of temperature and expression time, and different bacterial strains), we failed to obtain this mutant in the soluble state. Most of the MMM mutant was detected in the inclusion bodies (Figure S1 of the Supporting Information). Similar results were obtained with the WMM mutant of 14-3-3ζ [i.e., with the

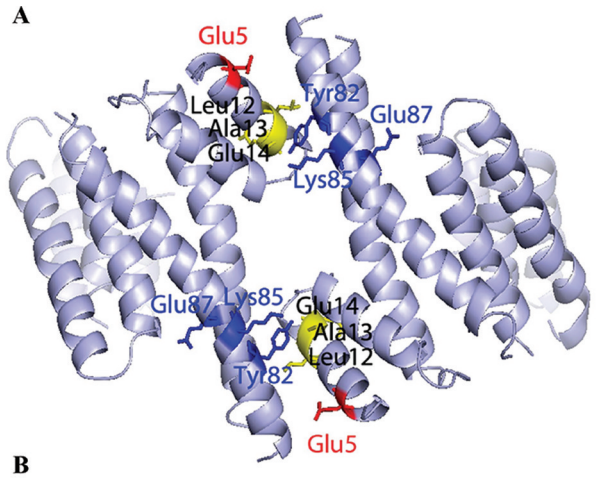

14-3-3ζ protein	Mutations at 14-3-3ζ dimer interface			Number of point mutations
	position 5	residues 12-14	residues 82-87	
MMM	K	QQR	QRENIQ	7
WMM	E	QQR	QRENIQ	6
MMW	K	QQR	YREKIE	4
WMW	E	QQR	YREKIE	3
WWW (WT)	E	LAE	YREKIE	0

Figure 1. Design of dimer-deficient mutants of the 14-3-3ζ. (A) Position of residues located on the dimer interface of 14-3-3ζ and mutated by Tzivion et al.[14] to produce the MMM monomeric mutant of 14-3-3. An image was built with PyMol version 1.1 using the data from Protein Data Bank entry 1A4O. Mutated residues are located in three sequences: residue 5, residues 12−14, and residues 82−87. The C-terminus of 14-3-3ζ is not shown because of its flexibility and its absence on the density maps. (B) Nomenclature for dimer-deficient 14-3-3ζ mutants. Mutated residues are underlined.

mutant containing a wild-type E at position 5 and mutated sequences at positions 12−14 and 82−87 (see Figure 1)]. Thus, both MMM and WMM mutants of 14-3-3 could not be properly folded in the bacterial system. Trying to improve solubility, we left the sequence at positions 82−87 unmutated and obtained the so-called WMW and MMW mutants (Figure 1). These mutants were successfully expressed in a soluble form in *E. coli*, purified to homogeneity, and used to investigate the structure and physicochemical properties of the putative monomeric forms of 14-3-3.

Biochemical Properties of Dimer-Deficient Mutants of 14-3-3ζ. The far-UV CD spectroscopy data (Figure S2 of the Supporting Information) indicate that the secondary structure of MMW and WMW mutants is indistinguishable from that of the wild-type protein. This suggests that the introduced mutations did not affect the proper folding of the analyzed proteins as judged by the high content of helical structure that was preserved.

In the WMW mutant, E^{14} is replaced with R, and in the MMW mutant, E^{5} is replaced with K and E^{14} with R (see Figure 1). Therefore, we may expect that these mutations would affect the isoelectric point of mutated 14-3-3. Indeed, the results of the isoelectric focusing performed under denaturing conditions indicate that the pI value of wild-type 14-3-3ζ is equal to 4.55, while the pI values of the WMW and MMW mutants are equal to 4.70 and 4.85, respectively (Figure S3 of the Supporting Information). Thus, introduced mutations change the charge in the N-terminal part of the molecule.

As mentioned earlier, phosphorylation of Ser58 or its phosphomimicking mutation (S58E) induces only partial dissociation of 14-3-3 dimers, which was observed only at a rather low protein concentration.[8] Therefore, it seemed reasonable to analyze the effect of the introduced mutations on the oligomeric state of 14-3-3 over a wide range of protein concentrations. Size-exclusion chromatography showed that wild-type 14-3-3 was eluted from the Superdex 200 column as a peak with a Stokes radius of 36.6 ± 0.1 Å in a manner independent of its concentration (Figure 2A). These data correlate well with our previous results and indicate that under the conditions used wild-type 14-3-3 exists as a dimer. In contrast, the Stokes radius of S58E 14-3-3 depended on the protein concentration.[8] At a low protein concentration, it was close to 32 Å, whereas at a high protein concentration, it was close to 36 Å. These data agree with our previous results and indicate that at a low protein concentration the dimer of S58E undergoes partial dissociation.[8] In contrast, the MMW and WMW mutants were eluted as peaks with a Stokes radius of 28.2 ± 0.2 Å, which presumably corresponds to a monomeric form of 14-3-3. This was confirmed by SEC-MALLS that showed that, in a manner independent of loaded protein concentration (0.5−6.0 mg/mL), WMW and MMW mutants were eluted as symmetrical peaks with a molecular mass of 28.4 ± 0.3 kDa and polydispersity index (PDI, or M_w/M_n) of only 1%. An example of the elution profile of the WMW mutant loaded on the column at a concentration of 3 mg/mL is presented in Figure 2B. The

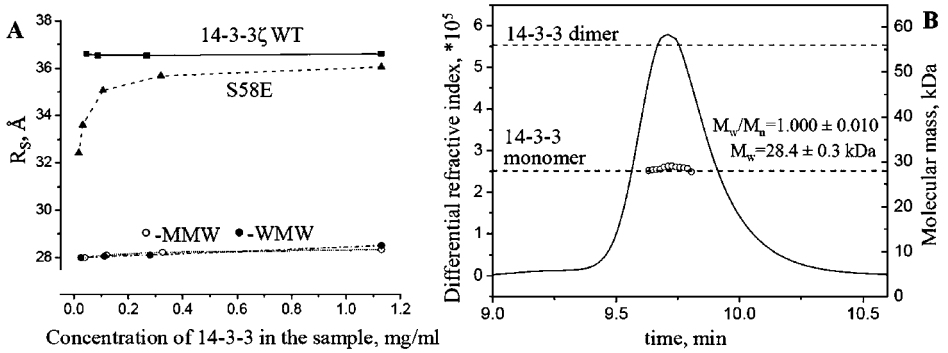

Figure 2. Hydrodynamic properties and oligomeric structure of WT 14-3-3ζ and its WMW and MMW mutants. (A) WT 14-3-3ζ or its mutants at different protein concentrations in the loading sample (0.01−1.15 mg/mL) were subjected to analytical size-exclusion chromatography on a calibrated Superdex 200 HR column. The column was operated at a flow rate of 0.5 mL/min. (B) SEC-MALLS experiment with the WMW mutant (3 mg/mL). Empty circles demonstrate the distribution of particle size with the indicated molecular mass (right axis) eluted in the peak of the WMW mutant obtained as a dependence of differential refractive index vs time (left axis). Dashed lines show theoretically calculated molecular masses of the dimer and monomer of 14-3-3. M_w/M_n represents the polydispersity index (PDI).

dx.doi.org/10.1021/bi201374s | *Biochemistry* 2011, 50, 9797−9808

calculated molecular mass of the 14-3-3ζ monomer is 27.75 kDa (http://www.uniprot.org/uniprot/P63104), very close to the experimentally determined values for WMW and MMW mutants. This allows to conclude that both WMW and MMW mutants exist in the monomeric form over a very wide range of concentrations. Significantly, CD spectroscopy data indicated that the mutations do not affect the secondary structure, suggesting these mutant proteins are suitable for investigating the structure and properties of the monomeric state of 14-3-3.

A priori, one can predict that disassembly of an oligomeric protein will be accompanied by exposure of interface buried sites or by changes in the surface hydrophobicity or stability of the liberated monomers. Indeed, our earlier results indicate that the phospho-mimicking S58E mutation leading to partial dissociation of the 14-3-3 dimer is accompanied by changes in hydrophobicity.[8] Because WMW and MMW mutants were completely monomeric, it seemed reasonable to analyze the effect of monomerization on the exposure of protein fluorophores and the overall protein hydrophobicity.

Recording the intrinsic Trp fluorescence excited at 295 nm, we found that the maximum of fluorescence of wild-type 14-3-3 was located at 342 nm, whereas fluorescence maxima of WMW and MMW mutants were located at 346 and 348 nm, respectively (Figure S4A of the Supporting Information). At the same time, the amplitude of intrinsic fluorescence of the WMW (133.7 ± 10.9%) and MMW (147.0 ± 2.9%) mutants was larger than that of the wild-type protein (100.0 ± 2.4%) (Figure S4B of the Supporting Information). Usually, the red shift of Trp fluorescence indicates the increased level of exposure of protein fluorophore to the solvent.[40] Recently published data indicated that a conservative Trp59 located at the dimer interface was mainly responsible for the intrinsic fluorescence of 14-3-3.[41] Therefore, our experimental data agree with the suggestion that dimer dissociation results in the exposure of Trp residues of 14-3-3 to the solvent. An unexpected increase in the intrinsic fluorescence of WMW and MMW mutants could be due to dissociation-induced changes in the structure and removal of the quenching residues.

It is well accepted that certain hydrophobic contacts are important for stabilization of the 14-3-3 dimer.[5,7] Therefore, it can be expected that monomerization could lead to the exposure of the interface-buried hydrophobic residues to the surface of 14-3-3 mutants. Titration of wild-type 14-3-3ζ with hydrophobic probe bis-ANS resulted in a moderate hyperbolic increase in fluorescence excited at 385 nm and recorded at 495 nm (Figure 3A). This reflected a rather tight binding of the hydrophobic probe to a restricted number of hydrophobic sites. In contrast, titration of MWW of WMW mutants with bis-ANS resulted in a practically linear increase of fluorescence that was significantly larger than for the wild-type protein (Figure 3A). This titration reflects binding of bis-ANS to a large number of low-affinity hydrophobic sites. Indeed, if the number of low-affinity bis-ANS binding sites is rather large and at the same time their affinity is low, then saturation (i.e., deviation from the linear titration curve) will be achieved only at a very high bis-ANS concentration, which cannot be achieved experimentally because of intrinsic quenching induced by addition of large quantities of bis-ANS. These results agree with a suggestion that monomerization leads to the exposure of a large number of hydrophobic sites, and this effect was more pronounced in the case of MMW than in the case of the WMW mutant (Figure 3A). This might be due to more effective

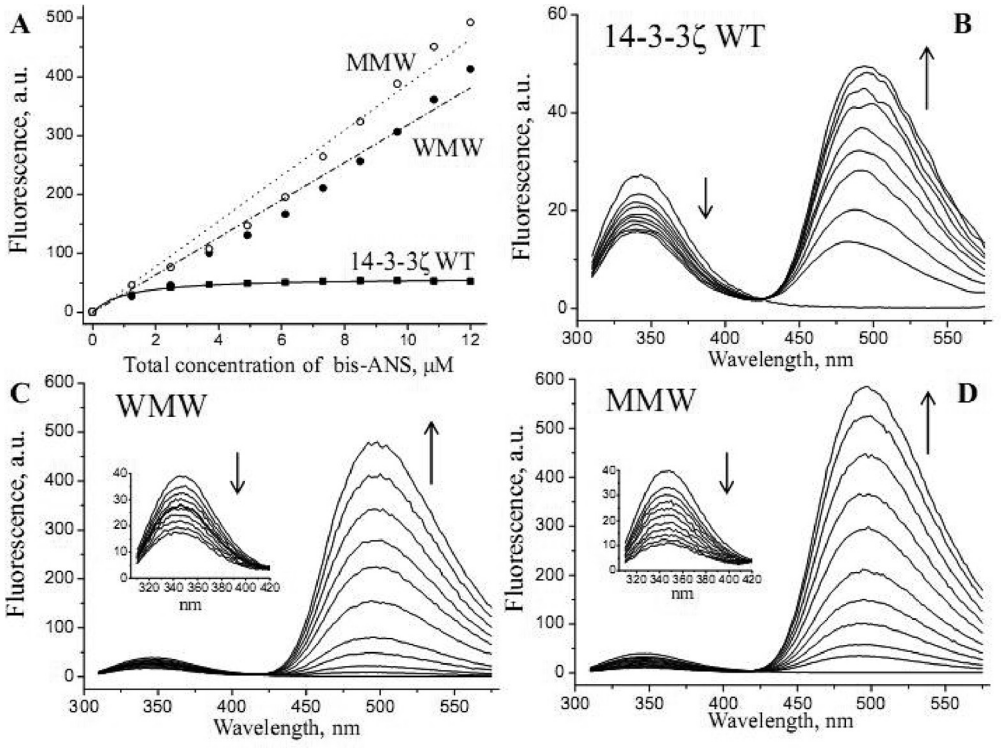

Figure 3. Bis-ANS binding to different 14-3-3ζ species. (A) Titration of 14-3-3 (1 μM) with increasing concentrations of bis-ANS (0−12 μM) as measured by the increase in fluorescence at 495 nm excited at 385 nm. Curves are corrected for the fluorescence of free bis-ANS. (B−D) FRET from Trp residues of 14-3-3 to bound bis-ANS recorded during the course of titration shown in panel A (excitation at 295 nm). Insets of panels C and D contain scaled-up Trp fluorescence spectra of WMW (C) and MMW (D) mutants in the course of titration. Arrows indicate the direction of changes in fluorescence upon titration.

dx.doi.org/10.1021/bi201374s | *Biochemistry* 2011, 50, 9797−9808

binding of negatively charged bis-ANS to the MMW mutant carrying a larger positive charge than the WMW mutant. Titration of 14-3-3 with bis-ANS resulted not only in a fluorescence increase at 495 nm but also in a fluorescence decrease at 340 nm (Figure 3B–D). This effect is due to the fluorescence resonance energy transfer (FRET) from excited Trp residues to bis-ANS bound in their vicinity. Titration of WMW and MMW monomeric mutants of 14-3-3 with bis-ANS produced a slightly more pronounced decrease in fluorescence at 340 nm (Figure 3B–D) and a much more significant increase in fluorescence at 495 nm compared with that of the wild-type protein. In summary, these results indicate that MMW and WMW mutants contain a large number of hydrophobic sites that are most probably buried in the case of a dimeric wild-type 14-3-3. Increased hydrophobicity of monomeric 14-3-3 might be an important prerequisite for its interaction with certain target proteins and for its potential chaperone-like activity.

Dissociation of 14-3-3 dimers can be accompanied by exposure of certain sites and destabilization of the monomer. To test this hypothesis, we analyzed the thermal stability of the wild-type protein and its mutants and their susceptibility to trypsinolysis. Following the dependence of intrinsic fluorescence on temperature, one can determine the temperature of half-transition from the folded to unfolded state and thus estimate the thermal stability of different proteins (see Materials and Methods and refs 8 and 35). Using this approach, we found that the half-transition temperature was 61.2 ± 0.4 °C for wild-type 14-3-3 and decreased to 59.0 ± 0.2 °C for the S58E mutant and 53.0 ± 0.9 and 52.6 ± 0.7 °C for WMW and MMW mutants, respectively (Figure S5 of the Supporting Information). These results indicate that partial dimer dissociation induced by the phospho-mimicking S58E mutation or complete dimer dissociation provoked by WMW or MMW mutations significantly decrease the thermal stability of 14-3-3.

Continuing this part of the investigation, we compared the kinetics of limited trypsinolysis for different 14-3-3 species (Figure 4). At a low ionic strength and in the presence of EDTA, wild-type 14-3-3ζ was resistant to trypsinolysis over a 90 min incubation, as the intensity of the 30 kDa band corresponding to the uncleaved protein remained essentially unchanged (Figure 4). Under identical conditions, the S58E mutant was less stable and its trypsinolysis resulted in a significant decrease in the intensity of the 30 kDa band and in the appearance of a new ~20 kDa band (Figure 4). WMW and especially MMW mutants were very unstable, and even a short (5–10 min) incubation with trypsin led to the complete disappearance of the 30 kDa band and rapid accumulation of the 20 kDa proteolytic product (Figure 4).

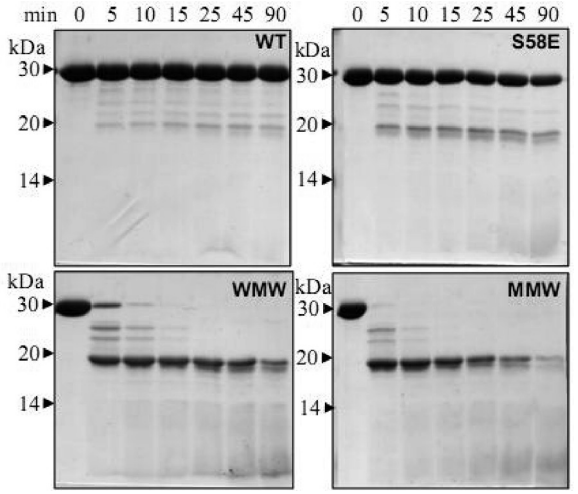

Figure 4. Limited trypsinolysis of wild-type 14-3-3ζ and its S58E, WMW, and MMW mutants in low-ionic strength buffer containing 3 mM EDTA. Trypsinolysis was performed at a 14-3-3:trypsin ratio equal to 150:1 at 37 °C. The duration of proteolysis (in minutes) is indicated above each lane. Positions of molecular mass markers (in kilodaltons) are shown by arrows.

In summary, the $E^5 \rightarrow K^5$ and $^{12}LAE^{14} \rightarrow {}^{12}QQR^{14}$ mutations (or even only $^{12}LAE^{14} \rightarrow {}^{12}QQR^{14}$) are sufficient to achieve complete monomerization of 14-3-3. These mutations do not affect the secondary structure of 14-3-3. However, these mutations lead to the changes in the electrical charge of the N-terminal portion and to exposure of new hydrophobic sites, which probably were buried in dimeric wild-type 14-3-3. Monomers of 14-3-3 are much less stable than the wild-type dimers to both thermal denaturation and trypsinolysis. Because monomerization results in significant changes in the properties of 14-3-3, interactions of the monomers with target proteins can be different from those of dimeric 14-3-3. Although the interactions of dimer-deficient mutants with different targets have been analyzed previously in several laboratories,[14,16,25,42,49] the results were somewhat contradictory, and many important questions remained unanswered. Moreover, dimer-deficient species of 14-3-3 described earlier either contained a very large number of point mutations (seven mutations in refs 14 and 16) or were lacking a rather large portion (~30 residues) of the N-terminal domain.[42,49] Therefore, we analyzed the interactions of different species of 14-3-3 with two model protein targets, namely, with the fetal isoform of human tau protein and human small heat shock protein HspB6 (Hsp20).

Interaction of 14-3-3ζ Monomers with Human Fetal Tau Protein. 14-3-3 might serve as an important partner of neuronal specific microtubule-associated tau protein,[4,30,43–45] and phosphorylation of tau protein at specific sites catalyzed by protein kinase A[45] and/or protein kinase B[44] enhances its interaction with 14-3-3.[30,44] Earlier, we found that the phospho-mimicking S58E mutation inducing partial dissociation of 14-3-3ζ weakened the interactions of 14-3-3 with phosphorylated tau, which allowed us to suggest that the monomers of 14-3-3 interacted with phosphorylated tau protein weaker than the intact dimers.[28] To test this hypothesis, we analyzed the interaction of wild-type 14-3-3 and its WMW and MMW mutants with phosphorylated and unphosphorylated tau protein.

On the native gel electrophoresis, wild-type 14-3-3 and its WMW and MMW mutants migrated as single sharp bands (Figure 5A, lanes 1, 3, and 5). The electrophoretic mobility of dimeric wild-type 14-3-3 was much lower than that of the monomeric WMW and MMW mutants, and as expected, the MMW mutant carrying a smaller negative charge migrated slower than the WMW mutant (Figure 5A, lanes 3 and 5). As shown previously,[28,30] isolated tau protein having an alkaline pI value of 9.4 (calculated for UniProt entry P10636) did not enter the gel and remained at the top independent of phosphorylation. When the mixture of unphosphorylated tau and wild-type 14-3-3 was loaded on the gel, we observed only the band corresponding to isolated 14-3-3 and a barely perceptible band of isolated tau remaining at the top of the gel (Figure 5A). However, if the mixture of phosphorylated tau

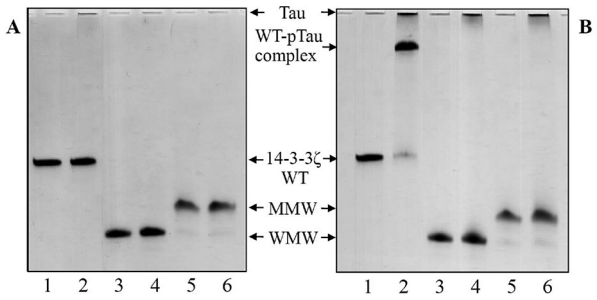

Figure 5. Interaction of WT 14-3-3ζ and its WMW and MMW mutants (5 μM) with unphosphorylated (A) or phosphorylated (B) by protein kinase A tau protein (8 μM) analyzed by means of native gel electrophoresis. Isolated wild-type 14-3-3ζ (1), WMW (3), and MMW (5) alone or a mixture of wild-type 14-3-3 and tau (2), WMW mutant and tau (4), or MMW mutant and tau (6) was subjected to native gel electrophoresis at pH 8.5. Tau protein because of its high pI remained on the top of the gel. The positions of wild-type 14-3-3 and its mutants (WMW and MMW) and the position of the complex of 14-3-3 and phosphorylated tau are shown by arrows.

and wild-type 14-3-3 was subjected to native gel electrophoresis, we detected a new band having electrophoretic mobility intermediate between those of tau protein and 14-3-3 (Figure 5B, lane 2). As shown previously,[45] this band contains a complex of 14-3-3 and phosphorylated tau. When similar experiments were performed with WMW and MMW mutants, we failed to detect formation of the new bands different from those of 14-3-3 and tau protein (Figure 5A,B, lanes 4 and 6). These data indicate that monomeric WMW and MMW mutants of 14-3-3 either do not interact or interact only very weakly with both phosphorylated and unphosphorylated tau protein.

To investigate further the interaction of different 14-3-3 species with tau protein, we used chemical cross-linking. Incubation of isolated wild-type 14-3-3 with glutaraldehyde (GA) led to the formation of cross-linked dimers with apparent molecular masses of 60 kDa (Figure 6A,B, lanes 1 and 2). At the same time, if WMW and MMW mutants were treated with GA, we observed formation of only trace amounts of the dimers (Figure 6A). In good agreement with previously presented data, this indicates that WMW and MMW mutants exist as monomers and are unable to form stable dimers. In our experimental setup, the treatment with GA did not lead to formation of cross-linked oligomers of tau, which probably underwent only intramolecular cross-linking (Figure 6B,C, lanes 3 and 4). Cross-linking of the mixture of wild-type 14-3-3ζ with phosphorylated tau protein resulted in the appearance of new ∼80 and ∼120−150 kDa bands, presumably corresponding to the 14-3-3·tau complexes with a stoichiometry equal to 1:1 (80 kDa) and 2:1−2:2 complexes (120 and 150 kDa), respectively (Figure 6B,C, lane 5). If WMW or MMW mutants were subjected to cross-linking with phosphorylated tau, we detected formation of only one new 80 kDa band corresponding to the 14-3-3·tau complex with a stoichiometry of 1:1 (Figure 6B,C, lanes 6 and 7). However, WMW and MMW mutants were unable to form 14-3-3·tau complexes with a 2:1 or 2:2 stoichiometry detected in the case of the wild-type protein. It seems possible that the 14-3-3·tau complexes with a stoichiometry 1:1 are less stable than the complexes with a stoichiometry 2:1 or 2:2, and therefore, we were unable to detect complexes formed by WMW or MMW mutants with phosphorylated tau via native gel electrophoresis (Figure 5B, lanes 4 and 6). Thus, the level of monomerization significantly weakens (but does not completely prevent) interaction of 14-3-3 with phosphorylated tau.

Interaction of 14-3-3ζ Monomers with Human HspB6 (Hsp20). It has been reported that wild-type 14-3-3 tightly interacts with the phosphorylated peptide of HspB6[46] and with intact phosphorylated HspB6,[38,47] and this interaction could be important for the regulation of non-muscle motility and smooth muscle contraction.[47] Our previous data indicated that the S58E mutation weakens the interaction of 14-3-3ζ with phosphorylated HspB6.[28] This is likely due to either the direct effect of the Ser58 mutation on HspB6 binding or the partial dissociation of 14-3-3 dimers induced by the S58E mutation. Therefore, it seemed desirable to conduct a detailed investigation of interaction between fully monomeric mutant forms of 14-3-3ζ and phosphorylated and unphosphorylated HspB6.

We used the method of native gel electrophoresis to determine whether monomeric WMW and MMW mutants of 14-3-3 interacted with HspB6. All experiments were performed with inclusion of 1 mM magnesium in the gel and running buffers because only under these conditions we were able to detect interaction of wild-type 14-3-3 with HspB6.[28] Addition of magnesium prevented dissociation of the S58E mutant,[28] and therefore, under the conditions that were used, electrophoretic mobilities of wild-type 14-3-3 and its S58E mutant were similar (Figure 7A, lanes 1 and 2). Monomeric WMW and MMW mutants had higher electrophoretic mobilities than dimeric wild-type 14-3-3 (Figure 7A, lanes 3 and 4). The

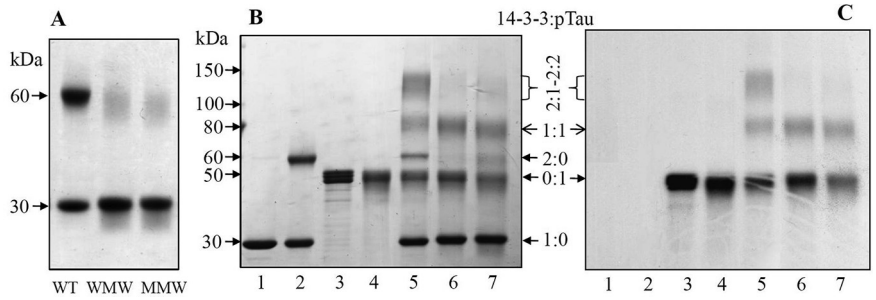

Figure 6. Chemical cross-linking of different species of WT 14-3-3ζ (10 μM) with phosphorylated tau protein (7 μM). (A) Cross-linking of isolated wild-type 14-3-3ζ and its WMW and MMW mutants with 0.05% glutaraldehyde. (B) Un-cross-linked (1) and cross-linked (2) wild-type 14-3-3ζ, un-cross-linked (3) and cross-linked (4) phosphorylated tau, or cross-linked mixtures of phosphorylated tau protein and wild-type 14-3-3 (5) or its WMW (6) and MMW (7) mutants were subjected to gradient (5 to 20%) SDS−PAGE. (C) Autoradiogram of the gel presented in panel B. Positions of the 14-3-3 monomer (1:0), 14-3-3 dimer (2:0), tau protein (0:1), and molecular mass markers are shown by closed arrows. Positions of the complexes of 14-3-3 with tau protein (1:1 and 2:1 to 2:2) are shown by open and figured arrows, respectively.

dx.doi.org/10.1021/bi201374s | Biochemistry 2011, 50, 9797−9808

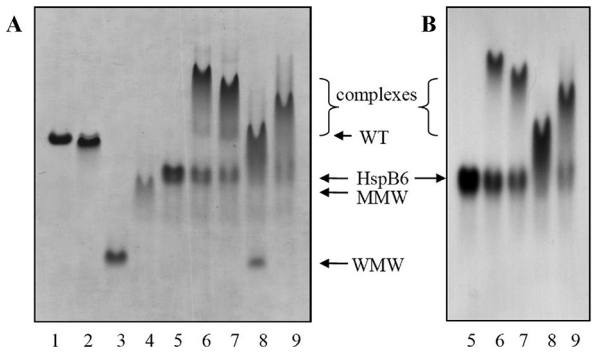

Figure 7. Interaction of different 14-3-3 species with phosphorylated HspB6 analyzed by means of native gel electrophoresis. Isolated wild-type 14-3-3 (1), its S58E (2), WMW (3), and MMW (4) mutants, isolated HspB6 (5), or an equimolar mixture of wild-type 14-3-3 and HspB6 (6), the S58E mutant and HspB6 (7), the WMW mutant and HspB6 (8), or the MMW mutant and HspB6 (9) was subjected to native 18% polyacrylamide gel electrophoresis in the presence of 1 mM $MgCl_2$. Panel A shows the Coomassie R-250-stained gel, and panel B shows the autoradiography of the same gel. Positions of different proteins and complexes are marked by arrows.

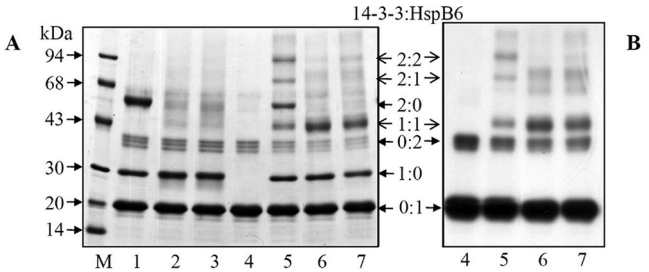

Figure 8. Chemical cross-linking of different 14-3-3 species and HspB6. A mixture of unphosphorylated HspB6 (0.3 mg/mL) and different species of 14-3-3 (0.15 mg/mL) (1−3) or isolated phosphorylated HspB6 (4) or a mixture of phosphorylated HspB6 (0.3 mg/mL) and different species of 14-3-3 (0.15 mg/mL) (5−7) was cross-linked by 0.05% glutaraldehyde followed by gradient (5 to 20%) SDS−PAGE (A) and autoradiography (B). The mixture of unphosphorylated HspB6 with wild-type 14-3-3 (1) or its WMW (2) or MMW (3) mutant, isolated phosphorylated HspB6 (4), or a mixture of phosphorylated HspB6 with wild-type 14-3-3 (5) or its WMW (6) or MMW (7) mutant was loaded on the gel. Heavy arrows indicate positions of monomers and homodimers of 14-3-3 and HspB6, and light arrows indicate positions of complexes with 14-3-3:HspB6 stoichiometries of 1:1, 2:1, and 2:2. Positions of the molecular mass standards (in kilodaltons) are indicated on the left.

increased duration of electrophoresis (18 h at room temperature) used in this set of experiments was accompanied by formation of more diffuse bands of WMW and MMW mutants (Figure 7A, lanes 3 and 4) than in the case of a short (2 h at room temperature) electrophoresis run in the absence of magnesium (Figure 5). The electrophoretic mobility of phosphorylated HspB6 was close to that of the MMW mutant (Figure 7A, lane 5). When mixtures of different species of 14-3-3 and phosphorylated HspB6 were loaded on the gel, new rather diffuse bands with electrophoretic mobilities lower than those of any single protein partners were detected (Figure 7). Formation of these bands was accompanied by a decrease in the intensity of the bands corresponding to isolated 14-3-3 and isolated HspB6. Moreover, the slowly migrating bands contained radioactivity belonging to phosphorylated HspB6 (Figure 7B), and their analysis via SDS gel electrophoresis revealed the presence of both 14-3-3 and HspB6 (data not shown). These observations indicate that monomeric mutants of 14-3-3 interact with phosphorylated HspB6. This interaction seems to be specific because it was observed only in the case of phosphorylated HspB6 and only if the electrophoresis was conducted in the presence of magnesium. In the absence of magnesium, both unphosphorylated HspB6 and phosphorylated HspB6 were unable to interact with any 14-3-3 species (data not shown).

The method of chemical cross-linking was used for further characterization of the complexes formed by 14-3-3 and HspB6. Cross-linking of the mixture of unphosphorylated HspB6 and wild-type 14-3-3 revealed four band groups with apparent molecular masses ∼20 and 30 kDa (corresponding to monomers of HspB6 and WT 14-3-3ζ, respectively) and 40 and 60 kDa (corresponding to cross-linked dimers of HspB6 and WT 14-3-3, respectively) (Figure 8A, lane 1). Cross-linked HspB6 migrated in the form of three closely separated faint bands with apparent molecular masses close to 40 kDa. These three bands probably correspond to HspB6 dimers cross-linked by glutaraldehyde at different sites and therefore with different counter lengths and possessing slightly different mobilities on the SDS gel electrophoresis. Cross-linking of the mixture of the WMW (or MMW) mutant with unphosphorylated HspB6 revealed the same bands except the 60 kDa band corresponding to a dimer of 14-3-3 (Figure 8A, lanes 2 and 3). If phosphorylated HspB6 was cross-linked to wild-type 14-3-3, then in addition to the four bands mentioned above we detected new bands with apparent molecular masses of ∼50, 80, and 100 kDa, which probably correspond to the cross-linked complexes with 14-3-3:HspB6 stoichiometries equal to 1:1, 2:1, and 2:2, respectively (Figure 8, lane 5). Only one additional 50 kDa band was detected when either the WMW mutant or the MMW mutant was cross-linked to phosphorylated HspB6 (Figure 8, lanes 6 and 7). These results indicate that monomeric WMW and MMW mutants predominantly form complexes with phosphorylated HspB6 with a 14-3-3:HspB6 stoichiometry of 1:1, whereas dimeric wild-type 14-3-3 can additionally form complexes with 14-3-3:HspB6 stoichiometries of 2:1 and 2:2.

For further characterization of the complexes formed by different species of 14-3-3 and HspB6, we used size-exclusion chromatography (SEC). Unphosphorylated HspB6 is unable to interact with any species of 14-3-3. Therefore, if the column was loaded with the mixture of unphosphorylated HspB6 and different species of 14-3-3, we observed well-separated peaks of isolated wild-type 14-3-3 and isolated HspB6, or an asymmetric merged peak of HspB6 and the WMW or MMW mutant (Figure 9A−C, solid lines). In all cases, the elution profile exactly corresponds to the sum of elution profiles of isolated proteins (Figure 9A−C, dashed lines), and in neither case were we able to detect any new peaks different from those of isolated 14-3-3 and isolated HspB6. When the mixture of phosphorylated HspB6 and 14-3-3 was loaded on the column, we detected a new peak with an elution volume smaller than that of the single proteins (Figure 9D−F). According to the data of SDS gel electrophoresis (data not shown and refs 28 and 38), this peak contained both 14-3-3 and HspB6. In the case of wild-type 14-3-3 and phosphorylated HspB6, the apparent molecular mass of the proteins eluted in this peak (elution volume around 13.7 mL) was in the range of 110−120 kDa, whereas in the case of WMW and MMW mutants and phosphorylated HspB6, the

dx.doi.org/10.1021/bi201374s | Biochemistry 2011, 50, 9797−9808

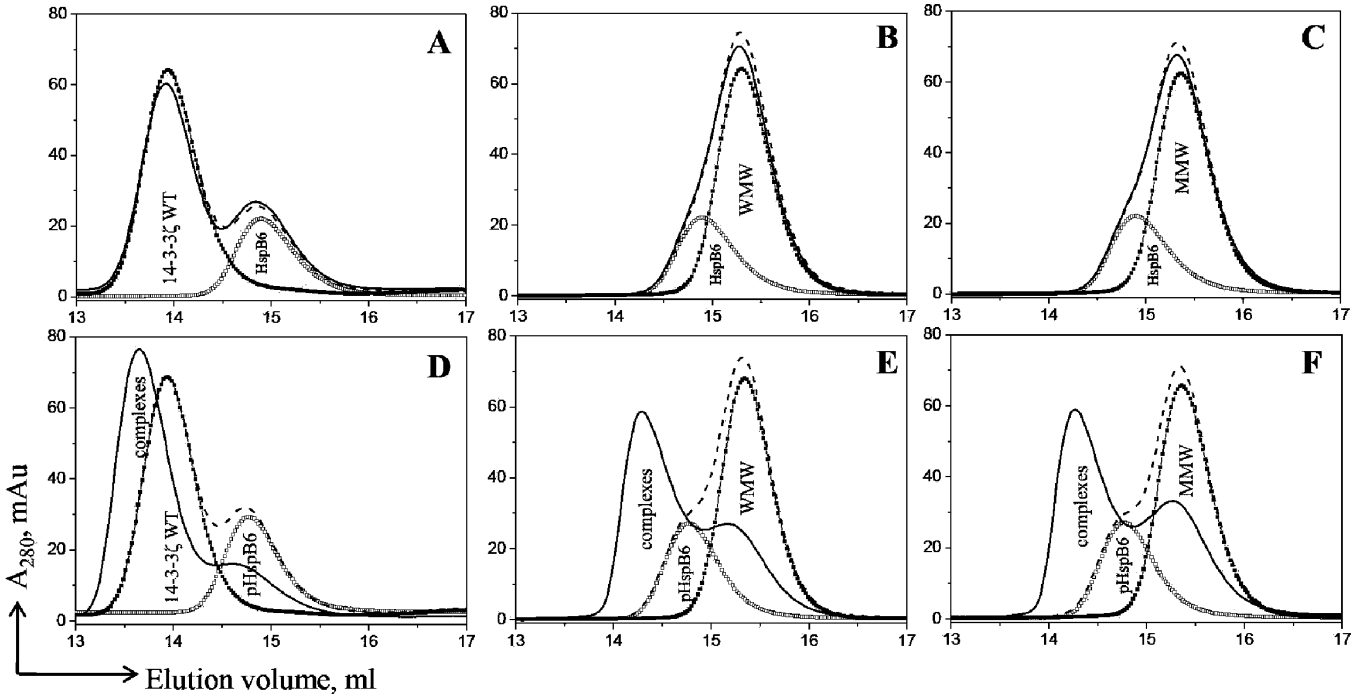

Figure 9. Size-exclusion chromatography of isolated HspB6, different species of 14-3-3, and their mixture on a Superdex 200 column. Isolated unphosphorylated (A–C) or phosphorylated (D–F) HspB6 (□), isolated wild-type 14-3-3 (A and D), the isolated WMW mutant (B and E), the isolated MMW mutant (C and F) (■), or their equimolar mixtures (—) were subjected to size-exclusion chromatography. Dashed lines represent the algebraic sum of elution profiles of isolated HspB6 and isolated 14-3-3 species. Positions of isolated proteins (HspB6 and different species of 14-3-3) and their complexes are indicated in each profile.

proteins eluted in this new peak (elution volume around 14.3 mL) had an apparent molecular mass of ~70 kDa. The apparent molecular masses determined by SEC for dimeric HspB6, dimeric WT 14-3-3ζ, and monomeric WMW (or MMW) mutants were 54, 80, and 40 kDa, respectively, suggesting that wild-type 14-3-3 forms a complex with phosphorylated HspB6 with a 14-3-3:HspB6 stoichiometry of 2:1 (80 + 27) or 2:2 (80 + 54), whereas WMW (and MMW) mutants form a complex with a stoichiometry of 1:1 (27 + 40).

To characterize the interactions of WMW and MMW mutants with phosphorylated HspB6, we estimated the apparent binding constants of these proteins. Fixed quantities of phosphorylated HspB6 were mixed with increasing amounts of wild-type 14-3-3 or its WMW or MMW mutants. Under the conditions used in the experiment, the peak of the isolated WMW (or MMW) mutant was well separated from the peak of isolated HspB6 (Figure S6 of the Supporting Information). Knowing the total concentrations of the 14-3-3 mutant and HspB6 and determining the concentration of the remaining free 14-3-3 mutant from the amplitude of the corresponding peak, we plotted the dependence of the $[HspB6_{bound}]/[HspB6_{total}]$ ratio versus the concentration of remaining free 14-3-3 and estimated the apparent binding constant.[48] A similar calculation could be done by analyzing the distribution of the radioactivity of phosphate bound to HspB6. This approach allowed us to estimate the apparent binding constant as 7.1 ± 2.1 μM for wild-type protein and 3.3 ± 1.3 and 4.9 ± 1.9 μM for WMW and MMW mutants, respectively. Thus, the affinity of monomeric mutants of 14-3-3 for phosphorylated HspB6 was similar or even slightly higher than the affinity of the wild-type protein.

In summary, we can conclude that the dimer-deficient WMW and MMW mutants specifically interact with phosphorylated HspB6 with an affinity comparable to (or even higher than) that of the wild-type protein. However, the stoichiometry of the complexes formed by the WMW and MMW mutants and phosphorylated HspB6 is close to 1:1, unlike complexes formed by wild-type 14-3-3, which have a stoichiometry of 2:1 or 2:2.

■ DISCUSSION

It is well-known that 14-3-3 proteins form stable homo- or heterodimers[5,21] and that the dimeric structure is of great importance for many physiologically important properties of 14-3-3, such as interaction and regulation of target proteins and scaffolding activity.[14,16,17] Formation of homo- and heterodimers can proceed only through tentative accumulation of monomers that later associate or participate in subunit exchange. Although monomers might be unstable and rapidly undergo dimerization, their concentration in certain cell lines with high levels of 14-3-3 expression might be perceptible. Moreover, recently published data indicate that under certain conditions (for instance, increased level of sphingosine or its derivatives) phosphorylation of Ser58 leads to partial dissociation of 14-3-3 dimers[20,22,23] and phosphorylation of other still poorly characterized sites[5,21] might further increase the probability of dissociation. Therefore, dimer dissociation and accumulation of monomers are supposed to be an important mechanism of regulation of 14-3-3 activity.[21−23] However, until now many biochemical properties of 14-3-3 monomers had not been analyzed in detail.

Two different approaches have been used to obtain monomeric forms of 14-3-3. The first approach involved truncation of certain regions in the N-terminal sequence of 14-3-3ζ.[42,49] These truncation mutants lacking the first N-terminal 32–78 residues were unable to form stable dimers. In addition, a new splicing variant of 14-3-3ε lacking the first 22 N-terminal

dx.doi.org/10.1021/bi201374s | Biochemistry 2011, 50, 9797–9808

residues and being unable to homodimerize and to form heterodimers with 14-3-3ζ has recently been described in the literature.[50] The structure and properties of such truncation mutants have not been characterized, and truncation of the first 32 residues weakened the interaction of 14-3-3ζ with the glycoprotein Ib-IX (GPIb-IX) complex without affecting its binding to the cytoplasmic domain of glycoprotein Ibα (GPIbα).[42] Deletion of the first 22 residues in a novel 14-3-3ε splicing variant does not affect protection of the HEK293 cell against UV irradiation-induced apoptosis.[50]

The second approach to obtaining the monomeric forms of 14-3-3, introduced by Tzivion et al.,[14] was based on mutation of three sequence motifs, namely, E5K, ^{12}LAE^{14} → ^{12}QQR^{14}, and ^{82}YREKIE^{87} → ^{82}QRENIQ^{87}. In the crystal structure,[7] these residues are located at the dimer interface, and therefore, mutations at these positions were predicted to induce dimer dissociation. Mutations of homologous residues in *Drosophila melanogaster* 14-3-3ζ (^{15}LAE^{17} → ^{15}QQR^{17} and ^{88}RVE^{90} → ^{88}NVQ^{90}) also led to its monomerization.[25,26] Like in the case of human 14-3-3ζ, the structure and physicochemical properties of these mutant proteins have not been characterized; however, it was postulated that mutations of one or both sequences in *Drosophila* 14-3-3ζ led to destabilization of its monomeric forms.[26] The data for the interaction of monomeric forms of 14-3-3 with target proteins are rather contradictory. For instance, monomeric forms of 14-3-3 were reported to interact with Raf kinase but were unable to regulate its activity.[14] Moreover, it has been postulated that monomeric forms of 14-3-3 interact with many target proteins in a nonspecific phosphorylation-independent manner.[16] It has also been reported that dimerization was important for stability and functioning of 14-3-3ζ in *Drosophila* neurons,[26] but at the same time, monomeric 14-3-3 was sufficient for modulating the activity of slowpoke calcium-dependent potassium channels of *Drosophila*.[25]

It is possible that some contradictory observations were due to insufficiently detailed information about the structure and properties of dimer-deficient mutants of 14-3-3. Our attempts to express MMM or WMM mutants of 14-3-3 in *E. coli* were unsuccessful because recombinant proteins were insoluble. This might indicate that extensive mutations addressing 14-3-3 monomerization might affect its proper folding. Therefore, we tried to minimize the number of mutations by producing the WMW and MMW monomeric mutant forms. Our data indicate that both mutants retained the α-helical structure of intact 14-3-3 (Figure S2 of the Supporting Information). However, both these mutants were highly susceptible to proteolysis (Figure 4) and had significantly reduced thermal stability (Figure S5 of the Supporting Information). These results support our proposal[8] and the hypothesis of Messaritou et al.[26] that monomeric forms of 14-3-3 are very unstable and can readily undergo degradation. If this conclusion is correct, then it is very difficult to make a correct comparison of diverse effects of intact dimeric and monomeric forms of 14-3-3 observed in different cell lines.

Our results indicate that monomerization results in significant changes in the hydrophobic properties of 14-3-3. This is not surprising because the intersubunit surface (~3000 Å^2 per monomer or ~30% of the total surface area of each subunit) contains seven hydrophobic residues of each subunit with exposed side chains (Met1, Leu12, Ala16, Val61, Val62, Ile65, and Tyr82) (calculated using Protein Data Bank entry 1A4O). Therefore, mutations inducing monomerization are expected to increase the hydrophobicity of 14-3-3 (Figure 3). The exposure of the hydrophobic residues normally buried in the dimer interface could provoke nonspecific aggregation of 14-3-3 monomers or could induce nonspecific interaction with different target proteins. Therefore, it seems highly probable that previously described interaction of 14-3-3 monomers with unphosphorylated proteins[16] could be the result of nonspecific hydrophobic binding of these proteins to the exposed hydrophobic surfaces of the monomer. To summarize, we conclude that a thorough analysis of the structure and folding of 14-3-3 monomers are required before proceeding with their functional studies in the cell. In addition, to reduce side effects of mutations, their number has to be kept to a minimum.

In this respect, our MMW and especially WMW mutants look really promising. Both mutant proteins remain monomeric over a wide range of protein concentrations and at the same time carry a minimal number of point mutations retaining many properties of wild-type 14-3-3. Our biophysical results indicate that the secondary structure of these mutants is indistinguishable from that of the wild-type protein. Moreover, these mutants specifically interact only with phosphorylated tau protein and HspB6, and in the latter case, the affinity of WMW and MMW mutants for phosphorylated HspB6 is comparable (if not higher) to the affinity of the wild-type protein. However, the monomeric mutants of 14-3-3 predominantly form 1:1 complexes with analyzed target proteins, whereas wild-type 14-3-3 forms 2:1 or 2:2 complexes with phosphorylated tau protein or phosphorylated HspB6. It is likely that the change in the stoichiometry of target binding upon monomerizaton will impact the cellular function of the 14-3-3 protein, which will be the subject of future investigations.

■ ASSOCIATED CONTENT

Ⓢ Supporting Information

Data for the expression of the 14-3-3ζ MMM mutant and its solubility (Figure S1), far-UV CD spectra of different species of 14-3-3 (Figure S2), isoelectric focusing of wild-type 14-3-3ζ and its mutants under denaturing conditions (Figure S3), intrinsic fluorescence of wild-type 14-3-3 and its dimer-deficient mutants (Figure S4), thermally induced changes in the Trp fluorescence of different 14-3-3 species (Figure S5), and titration of phosphorylated HspB6 with increasing quantities of the MMW mutant followed by SEC (Figure S6). This material is available free of charge via the Internet at http://pubs.acs.org.

■ AUTHOR INFORMATION

Corresponding Author

*Department of Biochemistry, School of Biology, Moscow State University, Moscow 119991 Russian Federation. Telephone fax: 7-495-939-2747. E-mail: NBGusev@mail.ru.

Funding

This investigation was supported by the Russian Foundation for Basic Science (Grant 10-04-00026) and the Wellcome Trust (Award 081916).

■ ACKNOWLEDGMENTS

We are grateful to Olga Moroz for her help in manuscript preparation, Callum Smits for his help with SEC-MALLS experiments, and Oleg Kovalevskiy for valuable discussions.

■ ABBREVIATIONS

S58E, phospho-mimicking mutant of 14-3-3ζ with Ser58 replaced with Glu; DTT, dithiothreitol; ME, β-mercaptoethanol; PKA, protein kinase A; SEC, size-exclusion chromatography; TPCK, tosyl-L-phenylalanine chloromethyl ketone; WT, wild type. WMM, WMW, MMW, and MMM designate the states of three regions inducing monomerization of 14-3-3 and marked either W (wild type) or M (mutated). In the first region, E^{5} was replaced with K^{5}; in the second region, $^{12}LAE^{14}$ were replaced with $^{12}QQR^{14}$, and in the third region, $^{82}YREKIE^{87}$ were replaced with $^{82}QRENIQ^{87}$.

■ REFERENCES

(1) Rittinger, K., Budman, J., Xu, J., Volinia, S., Cantley, L. C., Smerdon, S. J., Gamblin, S. J., and Yaffe, M. B. (1999) Structural analysis of 14-3-3 phosphopeptide complexes identifies a dual role for the nuclear export signal of 14-3-3 in ligand binding. *Mol. Cell 4*, 153−166.

(2) Coblitz, B., Wu, M., Shikano, S., and Li, M. (2006) C-terminal binding: An expanded repertoire and function of 14-3-3 proteins. *FEBS Lett. 580*, 1531−1535.

(3) Mackintosh, C. (2004) Dynamic interactions between 14-3-3 proteins and phosphoproteins regulate diverse cellular processes. *Biochem. J. 381*, 329−342.

(4) Sluchanko, N. N., and Gusev, N. B. (2010) 14-3-3 proteins and regulation of cytoskeleton. *Biochemistry (Moscow) 75*, 1528−1546.

(5) Gardino, A., Smerdon, S., and Yaffe, M. (2006) Structural determinants of 14-3-3 binding specificities and regulation of subcellular localization of 14-3-3-ligand complexes: A comparison of the X-ray crystal structures of all human 14-3-3 isoforms. *Semin. Cancer Biol. 16*, 173−182.

(6) Aitken, A. (2006) 14-3-3 proteins: A historic overview. *Semin. Cancer Biol. 16*, 162−172.

(7) Liu, D., Bienkowska, J., Petosa, C., Collier, R. J., Fu, H., and Liddington, R. (1995) Crystal structure of the ζ isoform of the 14-3-3 protein. *Nature 376*, 191−194.

(8) Sluchanko, N., Chernik, I., Seit-Nebi, A., Pivovarova, A., Levitsky, D., and Gusev, N. (2008) Effect of mutations mimicking phosphorylation on the structure and properties of human 14-3-3ζ. *Arch. Biochem. Biophys. 477*, 305−312.

(9) Robinson, K., Jones, D., Patel, Y., Martin, H., Madrazo, J., Martin, S., Howell, S., Elmore, M., Finnen, M. J., and Aitken, A. (1994) Mechanism of inhibition of protein kinase C by 14-3-3 isoforms. 14-3-3 isoforms do not have phospholipase A2 activity. *Biochem. J. 299*, 853−861.

(10) Muslin, A. J., Tanner, J. W., Allen, P. M., and Shaw, A. S. (1996) Interaction of 14-3-3 with signaling proteins is mediated by the recognition of phosphoserine. *Cell 84*, 889−897.

(11) Chun, J., Kwon, T., Lee, E. J., Kim, C. H., Han, Y. S., Hong, S. K., Hyun, S., and Kang, S. S. (2004) 14-3-3 protein mediates phosphorylation of microtubule-associated protein tau by serum- and glucocorticoid-induced protein kinase 1. *Mol. Cells 18*, 360−368.

(12) Mils, V., Baldin, V., Goubin, F., Pinta, I., Papin, C., Waye, M., Eychene, A., and Ducommun, B. (2000) Specific interaction between 14-3-3 isoforms and the human CDC25B phosphatase. *Oncogene 19*, 1257−1265.

(13) Yasmin, L., Jansson, A., Panahandeh, T., Palmer, R., Francis, M., and Hallberg, B. (2006) Delineation of exoenzyme S residues that mediate the interaction with 14-3-3 and its biological activity. *FEBS J. 273*, 638−646.

(14) Tzivion, G., Luo, Z., and Avruch, J. (1998) A dimeric 14-3-3 protein is an essential cofactor for Raf kinase activity. *Nature 394*, 88−92.

(15) Gu, Y.-M., Jin, Y.-H., Choi, J.-K., Baek, K.-H., Yeo, C.-Y., and Lee, K.-Y. (2006) Protein kinase A phosphorylates and regulates dimerization of 14-3-3ε. *FEBS Lett. 580*, 305−310.

(16) Shen, Y., Godlewski, J., Bronisz, A., Zhu, J., Comb, M., Avruch, J., and Tzivion, G. (2003) Significance of 14-3-3 self-dimerization for phosphorylation-dependent target binding. *Mol. Biol. Cell 14*, 4721−4733.

(17) Yaffe, M. (2002) How do 14-3-3 proteins work? Gatekeeper phosphorylation and the molecular anvil hypothesis. *FEBS Lett. 513*, 53−57.

(18) Megidish, T., Cooper, J., Zhang, L., Fu, H., and Hakomori, S. (1998) A novel sphingosine-dependent protein kinase (SDK1) specifically phosphorylates certain isoforms of 14-3-3 protein. *J. Biol. Chem. 273*, 21834−21845.

(19) Powell, D., Rane, M., Chen, Q., Singh, S., and McLeish, K. (2002) Identification of 14-3-3ζ as a protein kinase B/Akt substrate. *J. Biol. Chem. 277*, 21639−21642.

(20) Woodcock, J. M., Murphy, J., Stomski, F. C., Berndt, M. C., and Lopez, A. F. (2003) The dimeric versus monomeric status of 14-3-3ζ is controlled by phosphorylation of Ser58 at the dimer interface. *J. Biol. Chem. 278*, 36323−36327.

(21) Aitken, A. (2011) Post-translational modification of 14-3-3 isoforms and regulation of cellular function. *Semin. Cell Dev. Biol.*, DOI: doi: 10.1016/j.semcdb.2011.1008.1003.

(22) Kanno, T., and Nishizaki, T. (2010) Sphingosine induces apoptosis in hippocampal neurons and astrocytes by activating caspase-3/-9 via a mitochondrial pathway linked to SDK/14−3-3 Protein/Bax/Cytochrome c. *J. Cell. Physiol. 226*, 2329−2337.

(23) Woodcock, J. M., Ma, Y., Coolen, C., Pham, D., Jones, C., Lopez, A. F., and Pitson, S. M. (2010) Sphingosine and FTY720 directly bind pro-survival 14-3-3 proteins to regulate their function. *Cell. Signalling 22*, 1291−1299.

(24) Zhou, J., Shao, Z., Kerkela, R., Ichijo, H., Muslin, A., Pombo, C., and Force, T. (2009) Serine 58 of 14-3-3ζ is a molecular switch regulating ASK1 and oxidant stress-induced cell death. *Mol. Cell. Biol. 29*, 4167−4176.

(25) Zhou, Y., Reddy, S., Murrey, H., Fei, H., and Levitan, I. B. (2003) Monomeric 14-3-3 protein is sufficient to modulate the activity of the *Drosophila* slowpoke calcium-dependent potassium channel. *J. Biol. Chem. 278*, 10073−10080.

(26) Messaritou, G., Grammenoudi, S., and Skoulakis, E. M. (2010) Dimerization is essential for 14-3-3ζ stability and function in vivo. *J. Biol. Chem. 285*, 1692−1700.

(27) Sarkar, G., and Sommer, S. S. (1990) The "megaprimer" method of site-directed mutagenesis. *Biotechniques 8*, 404−407.

(28) Sluchanko, N. N., Sudnitsyna, M. V., Chernik, I. S., Seit-Nebi, A. S., and Gusev, N. B. (2011) Phosphomimicking mutations of human 14-3-3ζ affect its interaction with tau protein and small heat shock protein HspB6. *Arch. Biochem. Biophys. 506*, 24−34.

(29) Panasenko, O. O., Seit Nebi, A., Bukach, O. V., Marston, S. B., and Gusev, N. B. (2002) Structure and properties of avian small heat shock protein with molecular weight 25 kDa. *Biochim. Biophys. Acta 1601*, 64−74.

(30) Sluchanko, N., Seit-Nebi, A., and Gusev, N. (2009) Effect of phosphorylation on interaction of human tau protein with 14-3-3ζ. *Biochem. Biophys. Res. Commun. 379*, 990−994.

(31) Chung, C. T., Niemela, S. L., and Miller, R. H. (1989) One-step preparation of competent *Escherichia coli*: Transformation and storage of bacterial cells in the same solution. *Proc. Natl. Acad. Sci. U.S.A. 86*, 2172−2175.

(32) Studier, F. W. (2005) Protein production by auto-induction in high density shaking cultures. *Protein Expression Purif. 41*, 207−234.

(33) Laemmli, U. K. (1970) Cleavage of structural proteins during the assembly of the head of bacteriophage T4. *Nature 227*, 680−685.

(34) Bukach, O. V., Seit-Nebi, A. S., Marston, S. B., and Gusev, N. B. (2004) Some properties of human small heat shock protein Hsp20 (HspB6). *Eur. J. Biochem. 271*, 291−302.

(35) Bushueva, T. L., Busel, E. P., and Burstein, E. A. (1978) Relationship of thermal quenching of protein fluorescence to intramolecular structural mobility. *Biochim. Biophys. Acta 534*, 141−152.

(36) Kazakov, A. S., Markov, D. I., Gusev, N. B., and Levitsky, D. I. (2009) Thermally induced structural changes of intrinsically disordered small heat shock protein Hsp22. *Biophys. Chem. 145*, 79−85.
(37) Scott, C. W., Spreen, R. C., Herman, J. L., Chow, F. P., Davison, M. D., Young, J., and Caputo, C. B. (1993) Phosphorylation of recombinant tau by cAMP-dependent protein kinase. Identification of phosphorylation sites and effect on microtubule assembly. *J. Biol. Chem. 268*, 1166−1173.
(38) Chernik, I., Seit-Nebi, A., Marston, S., and Gusev, N. (2007) Small heat shock protein Hsp20 (HspB6) as a partner of 14-3-3γ. *Mol. Cell. Biochem. 295*, 9−17.
(39) Schaub, M. C., and Perry, S. V. (1969) The relaxing protein system of striated muscle. Resolution of the troponin complex into inhibitory and calcium ion-sensitizing factors and their relationship to tropomyosin. *Biochem. J. 115*, 993−1004.
(40) Burstein, E. A., Vedenkina, N. S., and Ivkova, M. N. (1973) Fluorescence and the location of tryptophan residues in protein molecules. *Photochem. Photobiol. 18*, 263−279.
(41) Bustad, H. J., Underhaug, J., Halskau, O. Jr., and Martinez, A. (2011) The binding of 14-3-3γ to membranes studied by intrinsic fluorescence spectroscopy. *FEBS Lett. 585*, 1163−1168.
(42) Gu, M., and Du, X. (1998) A novel ligand-binding site in the ζ-form 14-3-3 protein recognizing the platelet glycoprotein Ibα and distinct from the c-Raf-binding site. *J. Biol. Chem. 273*, 33465−33471.
(43) Hashiguchi, M., Sobue, K., and Paudel, H. K. (2000) 14-3-3ζ is an effector of tau protein phosphorylation. *J. Biol. Chem. 275*, 25247−25254.
(44) Sadik, G., Tanaka, T., Kato, K., Yamamori, H., Nessa, B. N., Morihara, T., and Takeda, M. (2009) Phosphorylation of tau at Ser214 mediates its interaction with 14-3-3 protein: Implications for the mechanism of tau aggregation. *J. Neurochem. 108*, 33−43.
(45) Sluchanko, N., Seit-Nebi, A., and Gusev, N. (2009) Phosphorylation of more than one site is required for tight interaction of human tau protein with 14-3-3ζ. *FEBS Lett. 583*, 2739−2742.
(46) Dreiza, C. M., Brophy, C. M., Komalavilas, P., Furnish, E. J., Joshi, L., Pallero, M. A., Murphy-Ullrich, J. E., von Rechenberg, M., Ho, Y. S., Richardson, B., Xu, N., Zhen, Y., Peltier, J. M., and Panitch, A. (2005) Transducible heat shock protein 20 (HSP20) phosphopeptide alters cytoskeletal dynamics. *FASEB J. 19*, 261−263.
(47) Dreiza, C. M., Komalavilas, P., Furnish, E. J., Flynn, C. R., Sheller, M. R., Smoke, C. C., Lopes, L. B., and Brophy, C. M. (2010) The small heat shock protein, HSPB6, in muscle function and disease. *Cell Stress Chaperones 15*, 1−11.
(48) Wilkinson, K. D. (2004) Quantitative analysis of protein-protein interactions. *Methods Mol. Biol. 261*, 15−32.
(49) Luo, Z. J., Zhang, X. F., Rapp, U., and Avruch, J. (1995) Identification of the 14.3.3 ζ domains important for self-association and Raf binding. *J. Biol. Chem. 270*, 23681−23687.
(50) Han, D., Ye, G., Liu, T., Chen, C., Yang, X., Wan, B., Pan, Y., and Yu, L. (2010) Functional identification of a novel 14-3-3ε splicing variant suggests dimerization is not necessary for 14-3-3ε to inhibit UV-induced apoptosis. *Biochem. Biophys. Res. Commun. 396*, 401−406.